Advanced Materials Research Vol. 854 (2014) pp 117-124
Online available since 2013/Nov/21 at www.scientific.net

doi:10.4028/www.scientific.net/AMR.854.117

Comparative investigation of structural and optical properties of Si-rich oxide films fabricated by magnetron sputtering

L. Khomenkova[1,a], M. Baran[1,b], O. Kolomys[1,c], V. Strelchuk[1,d], A. Kuchuk[1,e], V. Kladko[1,f], J. Jedrzejewski[2,g], I. Balberg[2,h], Y. Goldstein[2,i], Ph. Marie[3,j], F. Gourbilleau[3,k] and N. Korsunska[1,l]

[1]V. Lashkaryov Institute of Semiconductor Physics, 45 Pr. Nauky, 03028 Kyiv, Ukraine

[2]Racah Institute of Physics, Hebrew University, 91904 Jerusalem, Israel

[3]CIMAP, 6 Boulevard Marechal Juin, 14050 Caen, France

[a]khomen@isp.kiev.ua, [b]baran@isp.kiev.ua, [c]kolomys@isp.kiev.ua, [d]strelch@isp.kiev.ua, [e]kuchuk@isp.kiev.ua, [f]kladko@isp.kiev.ua, [g]jjedrzej@phys.huji.ac.il, [h]balberg@vms.huji.ac.il, [i]ygoldstein@vms.huji.ac.il, [j]philippe.marie@ensicaen.fr, [k]fabrice.gourbilleau@ensicaen.fr, [l]kors@isp.kiev.ua

Keywords: Silicon nanoclusters; RF magnetron sputtering; Photoluminescence; Raman scattering; Electron paramagnetic resonance

Abstract. RF magnetron sputtering of two separate silicon and oxide (SiO_2 or Al_2O_3) targets in pure argon plasma was used for deposition of $Si_x(SiO_2)_{1-x}$ and $Si_x(Al_2O_3)_{1-x}$ films with x=0.15-0.7 on long fused quarts substrate. The effect of post-fabrication treatments on structural and light emitting properties of the films with different *x* values was investigated by means of Raman scattering, electron paramagnetic resonance and X-ray diffraction as well as by photoluminescence (PL) methods. The formation of amorphous Si clusters upon deposition process was found for the both types of films. The annealing treatment at 1150°C during 30 min results in formation of Si nanocrystallites (Si-ncs). The latter were found to be larger in $Si_x(Al_2O_3)_{1-x}$ films than that in $Si_x(SiO_2)_{1-x}$ counterparts with the same *x* values and are under tensile stresses. The investigation of photoluminescence properties of annealed films of both types revealed the appearance of visible-near infrared light emission. The $Si_x(SiO_2)_{1-x}$ films demonstrated one broad PL band which peak position shifts gradually to from 1.4 eV to 1.8 eV with the *x* decrease. Contrary to this, for the $Si_x(Al_2O_3)_{1-x}$ films two overlapped PL bands were observed in the 1.4-2.4 eV spectral range with peak positions at ~2.1 eV and ~1.7 eV accompanied by near-infrared tail. Comparative analysis of PL spectra of both types' samples showed that the main contribution to PL spectra of $Si_x(SiO_2)_{1-x}$ films is given by exciton recombination in the Si-ncs whereas PL emission of $Si_x(Al_2O_3)_{1-x}$ films is caused mainly by carrier recombination either via defects in matrix or via electron states at the Si-ncs/matrix interface.

Introduction

One of the important tasks of photonics and microelectronics is realization of low-cost integrated optoelectronic devices fully based on well-developed Si-based CMOS technology (i.e. all-in-one Si chip). In this regard, silicon nanocrystallites (Si-ncs) attract considerable interest due to significant transformation of their optical and electrical properties caused by quantum-confinement effect [1-3].

Light-emitting Si-ncs embedded in dielectric hosts offer potential applications in optoelectronic devices because of their compatibility with the existing manufacturing infrastructure for silicon integrated circuits. Among different dielectric materials, silicon oxide is the most addressed as a

host for Si-ncs [4-7]. The properties of Si-ncs-SiO_2 systems have been widely investigated during last decades [2-8].

However, the downscaling of microelectronic devices requires the elaboration of novel materials to overcome bottleneck of silicon oxide as a gate material. In this regard, other dielectrics such as ZrO_2, HfO_2 and Al_2O_3 are considered as promising gate dielectrics [9]. It was also demonstrated that Si-ncs embedded in such high-k host offer a wider application for non-volatile memories due to the higher performance of the corresponding devices [10, 11].

Among different dielectrics, Al_2O_3 is not well addressed as photonic material. Meanwhile, it has relatively higher refractive index (1.73 at 1.95 eV) in comparison with that of SiO_2 (1.46 at 1.95 eV) at similar band gap energies offering better light confinement, making compact device structures possible. Recently, alumina-based waveguides have been developed by sol-gel techniques for optical communication. Only few groups reported on Si-ncs-Al_2O_3 materials fabricated by ion implantation or electron beam evaporation [12-14]. At the same time, magnetron sputtering was not often considered for fabrication of Al_2O_3 materials with embedded Si-ncs [15] in spite of the relative simplicity of this approach and its wide application for the fabrication of Si-ncs-SiO_2 films [5, 6].

The present paper demonstrates the application of magnetron sputtering for the fabrication of Si-rich-Al_2O_3 and Si-rich-SiO_2 films with different Si content. The study of the effect of post-deposition processing on the evolution of microstructure of the films and their optic and luminescent properties allowed to get information about the Si-ncs formation and the nature of the emitting centers in the films with different Si content as well as to find a way to control luminescent properties of these materials.

Experimental procedure

The $Si_x(Al_2O_3)_{1-x}$ and $Si_x(SiO_2)_{1-x}$ films with $0.15 \leq x \leq 0.7$ were deposited by radio frequency magnetron co-sputtering of two spaced-apart targets (pure Si and pure oxide (Al_2O_3 or SiO_2)) in pure argon plasma on a long silicon oxide substrate at room temperature. The films were grown on non-rotated substrate. Such approach permitted to vary excess Si content along the film length during one deposition run at fixed powers applied to the targets. The length and the width of the film were about 3 mm and 140 mm due to template use [19]. An annealing treatment of such long film gives the possibility to investigate simultaneous formation of the Si-ncs in the films with different Si excess.

The background vacuum in the chamber was about 1×10^{-5} Pa prior to the deposition. The RF power applied on SiO_2 and Al_2O_3 targets were 60 W and 80 W, respectively, whereas the power applied on Si cathode was 40 W for both cases. The deposition time was chosen to grow the films with the thickness of about 1 μm. The as-deposited original films were annealed at 1150°C during 30 min in nitrogen flow to form the Si-ncs in oxide hosts and then they were cut to smaller (1-cm in the length) segments (called hereafter as samples) to simplify the investigation of their properties.

To investigate the microstructure and luminescent properties of the films, a Horiba Jobin-Yvon T-64000 Raman spectrometer equipped with confocal microscope and automated piezo-driven XYZ stage was used. The measurements were performed at the center of each segment. The micro-Raman scattering (μ-RS) and micro-photoluminescence (μ-PL) spectra were detected in 100-900-cm^{-1} and in 500-900-nm spectral ranges, respectively. A 488.0-nm line of Ar-Kr ion laser was used as the excitation source. The laser power on the sample surface was always kept below 5 mW to obtain the best signal-to-noise ratio, preventing a laser heating of the investigated sample. The spectral resolution of the spectrometer was less than 0.15 cm^{-1}. X-ray diffraction (XRD) study was carried out using Philips X'Pert-MRD diffractometer with Cu K_α-radiation (λ=0.15418 nm) in a grazing geometry.

To study the chemical composition of the films (x), the spectroscopic ellipsometry measurement was performed by means of a Jobin-Yvon ellipsometer (UVISEL), where the incident light was scanned in the range 1.5-4.5 eV under an incident angle of 66.3°. The fitting of the experimental

data using DeltaPsi2 software [16] allowed to estimate variation of the refractive index versus along the film and based on the approach described in [9, 17] to estimate the *x* value. It is worth to note that obtained results were found to be in a good agreement with the data obtained by secondary mass spectrometry method for similar films [6]. The electron paramagnetic resonance (EPR) spectra were measured by means Varian-12 spectrometer to obtain the information about the defect structure of the samples. The investigations were performed at 300 K.

Results

Raman scattering spectra. Raman scattering signal was detected for as-deposited $Si_x(Al_2O_3)_{1-x}$ and $Si_x(SiO_2)_{1-x}$ films with the $x \geq 0.35$ and revealed the presence of amorphous silicon (a-Si) phase (Fig.1a). Besides, the shift of peak position of the transverse optic (TO) band to $\omega_{TO\text{-}a\text{-}Si}=460cm^{-1}$ was observed for $Si_x(Al_2O_3)_{1-x}$ films contrary to that detected for $Si_x(SiO_2)_{1-x}$ counterparts ($\omega_{TO\text{-}a\text{-}Si}=480cm^{-1}$). This latter corresponds to the TO phonon peak position of relaxed amorphous silicon. The low-frequency shift observed for $Si_x(Al_2O_3)_{1-x}$ samples can be ascribed to tensile stresses between the film and fused quarts substrate due to mismatching between lattice parameters of fused quarts and the film. It is obvious that this effect is negligible for the $Si_x(SiO_2)_{1-x}$ films.

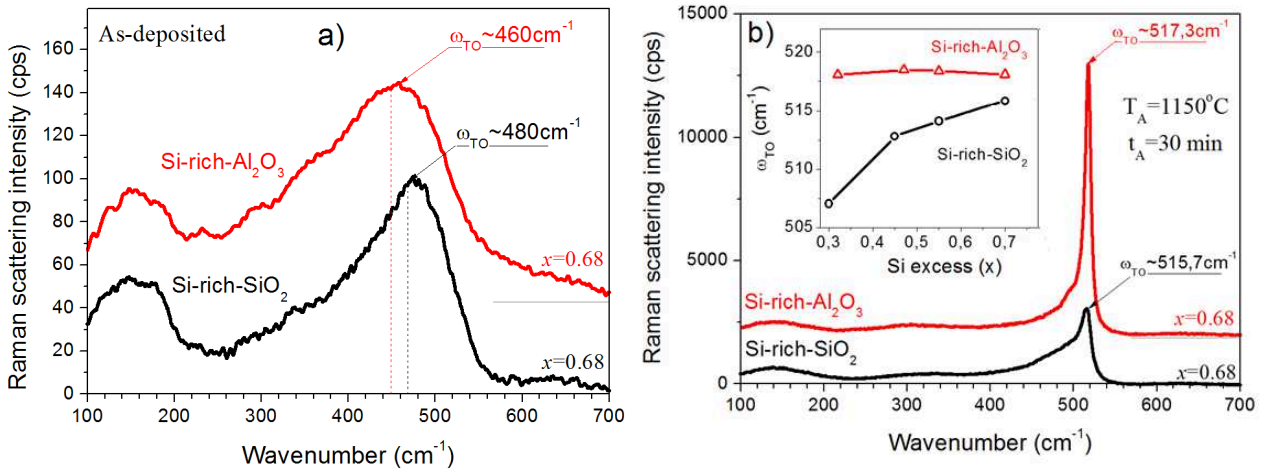

Fig.1. Raman scattering spectra as-deposited (a) and annealed (b) $Si_x(SiO_2)_{1-x}$ and $Si_x(Al_2O_3)_{1-x}$ films with x=0.68. The inset in Fig.1b shows variation of TO phonon peak position versus x for both types of samples.

Annealing treatment at T_A=1150°C results in the increase of TO phonon band intensity and its narrowing that is the evidence of Si-ncs formation in both types of the samples (Fig.1b). When the x decreases, the shift of the $\omega_{TO\text{-}nc\text{-}Si}$ to the lower wavenumbers occurs for $Si_x(SiO_2)_{1-x}$ (Fig.1b, inset) that can be ascribed to the decrease of Si-ncs sizes.

In all $Si_x(Al_2O_3)_{1-x}$ samples, the $\omega_{TO\text{-}nc\text{-}Si}$ is shifted to lower wavenumbers (517.3-518.7 cm^{-1}) in comparison with the peak position of TO phonon band of bulk Si ($\omega_{TO\text{-}bulk\text{-}Si}$=521 cm^{-1}). But contrary to $Si_x(SiO_2)_{1-x}$ films, for $Si_x(Al_2O_3)_{1-x}$ samples with x=0.55-0.7 only slight shift of the ω_{TO} towards the higher wavenumbers is detected with x decrease (Fig.1b, inset).

It is worth to note that along with Si crystalline phase, the amorphous Si phase was also detected in annealed samples. However, for the samples with the same x values its contribution is lower for the $Si_x(Al_2O_3)_{1-x}$ samples than for $Si_x(SiO_2)_{1-x}$ counterparts.

EPR study. The presence of amorphous Si phase in as-deposited samples was also revealed by EPR measurements. As one can see from Fig.2, the EPR spectra of the both types' samples with $x \geq 0.35$ are dominated by the signal with g=2.0055 (Fig.2) that corresponds to the silicon dangling bonds. Its intensity reflects the total number of these centers and decreases with x decrease.

Annealing treatment results in the transformation of EPR spectra of both types of samples. In $Si_x(SiO_2)_{1-x}$ films with x>0.35, an asymmetric signal with g=2.0057, which intensity increase with *x,* was found (Fig.2a). Besides, for the layers with *x*>0.55 slight dependence of EPR spectra on the orientation of magnetic field was detected. Since annealed $Si_x(SiO_2)_{1-x}$ films contain both Si-ncs and amorphous Si phase, this signal is obviously a superposition of two signals, i.e. P_b-like centers that are the feature of Si/SiO_2 interface formation, and Si dangling bonds. Slight anisotropy of EPR signal and the increase of the g-factor value are additional arguments for the formation of P_b-like centers.

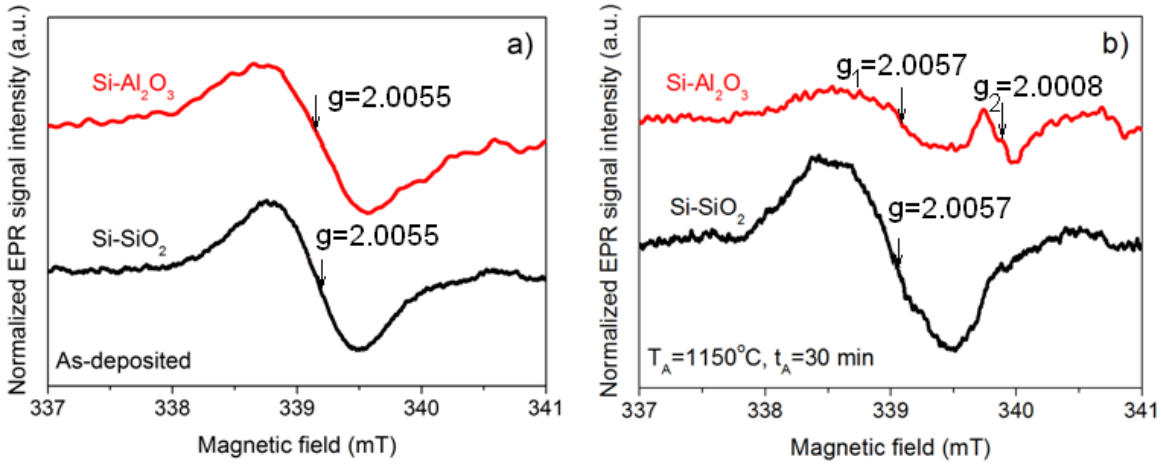

Fig. 2. Normalized EPR spectra of as-deposited (a) and annealed (b) $Si_x(SiO_2)_{1-x}$ and $Si_x(Al_2O_3)_{1-x}$ films with *x*=0.50.

Annealed $Si_x(Al_2O_3)_{1-x}$ samples showed two signals with g_1=2.0057 and g_2=2.0008 instead of single one with g=2.0055 detected for as-deposited films (Fig.2b). The first of these signals can be attributed to the superposition of Si dangling bonds and P_b-like centers that can be the feature of both Si/SiO_2 and Si/Al_2O_3 interfaces [18]. However, the nature of the second signal is still unclear yet. Its intensity decreases with the *x* decrease, but it is not detected for pure Al_2O_3 films. Therefore, it can be assumed that this EPR signal is due to some Si-related paramagnetic defects in Al_2O_3 host.

XRD patterns. XRD signal was detected for $Si_x(Al_2O_3)_{1-x}$ with x>0.5 and for $Si_x(SiO_2)_{1-x}$ with x>0.3 (Fig.3). The estimation of Si-ncs embedded in Al_2O_3 host based on the Scherrer equation were found to be about 14 nm for x>0.5 and did not vary with the *x* [19].

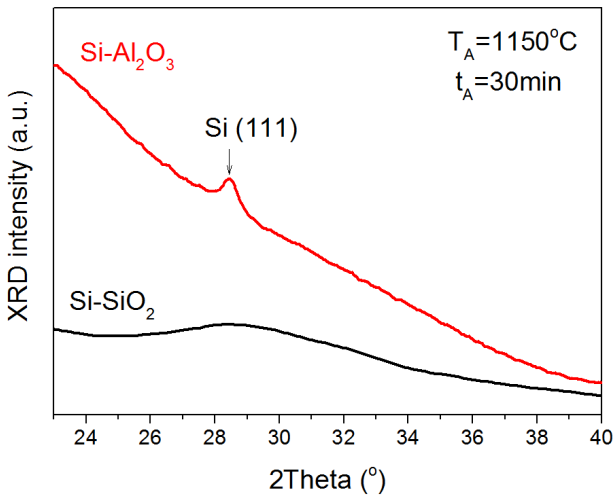

Fig. 3. XRD patterns of annealed $Si_x(SiO_2)_{1-x}$ and $Si_x(Al_2O_3)_{1-x}$ films with *x*=0.68

The Si-ncs formed in SiO_2 matrix were found to be smaller for the same x values. For $x>0.5$ their mean size was about 5-6 nm and did not change with x, whereas for $0.3<x<0.5$ the decrease of Si-ncs from 5 nm to 2.7 nm was observed with the x decrease.

Photoluminescence. Any emission was not observed for as-deposited $Si_x(SiO_2)_{1-x}$ films, whereas weak PL emission in orange spectral range was detected from $Si_x(Al_2O_3)_{1-x}$ films with $x<0.5$. Similar PL emission was also observed in pure Al_2O_3 film (Fig. 4b) and can be assigned to F_2^{2+} centers in Al_2O_3 [20].
Annealing of $Si_x(SiO_2)_{1-x}$ films results in the appearance of one broad PL band in red-near-infrared spectral range (Fig.4a). Its peak position shifts from 1.4 eV to 1.8 eV when the x decreases from 0.45 to 0.3 and does not change for $x>0.5$ (Fig.4a, inset).

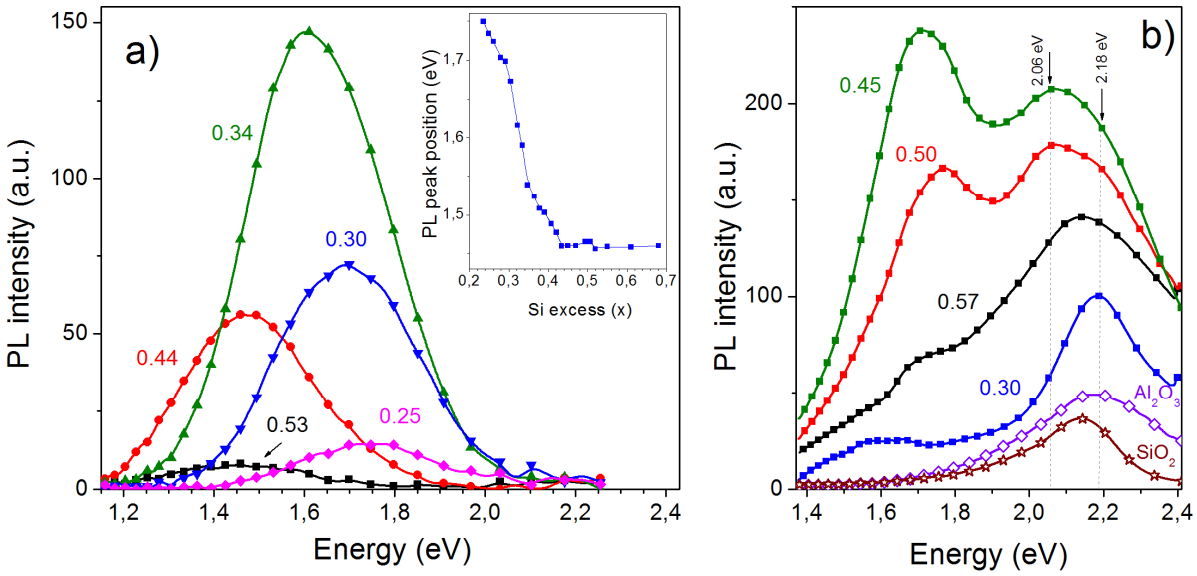

Fig. 4. Room-temperature PL spectra of $Si_x(SiO_2)_{1-x}$ (a) and $Si_x(Al_2O_3)_{1-x}$ (b) films. The values of the x are mentioned in the figures. Excitation wavelength is 488 nm.

Annealed $Si_x(Al_2O_3)_{1-x}$ films demonstrate the PL spectrum in wider spectral range (Fig.4b). These spectra contain two broad PL bands with maxima at 2.06-2.18 eV and 1.65-1.77 eV accompanied by near-infrared tail or weak band (1.55-1.60 eV). These bands can be well-separated (for x=0.45-0.5) or strongly overlapped. The first band consists of two components with maxima positions at ~2.06 eV and ~2.18 eV. The latter one is clearly seen in the sample with x=0.3 and is similar to PL emission from F_2^{2+} centers in Al_2O_3 [21]. Furthermore, this PL band presents in other spectra also, testifying that the Si-ncs are incorporated into Al_2O_3 matrix. At the same time, both components are strongly overlapped in the samples with $x>0.3$ (Fig.4).

Discussion

The investigation of structural properties of as-deposited $Si_x(SiO_2)_{1-x}$ and $Si_x(Al_2O_3)_{1-x}$ films showed that one of their specific features is the presence of amorphous Si phase for the samples with $x>0.35$ based on EPR data. Besides, the $Si_x(Al_2O_3)_{1-x}$ films are stressed contrary to $Si_x(SiO_2)_{1-x}$ ones. These stresses are tensile and caused by the mismatching in the lattice constants of fused quarts substrate and the film.

Comparison of XRD and Raman scattering data shows that after annealing treatment the Si-ncs in $Si_x(Al_2O_3)_{1-x}$ samples are stressed. In fact, the peak position of TO phonon band of the Si-ncs for the samples with $x>0.5$ is shifted to the lower frequency side ($\omega_{TO\text{-}nc\text{-}Si}$=517-518 cm^{-1}) in comparison with that for bulk Si ($\omega_{TO\text{-}bulk\text{-}Si}$=521 cm^{-1}). At the same time, the mean size of Si-ncs, estimated from XRD data, is about 14 nm. It is obvious that the contribution of phonon quantum

confinement effect is negligible in this case. This means that the Si-ncs in the $Si_x(Al_2O_3)_{1-x}$ samples are under tensile stress contrary to the Si-ncs in the $Si_x(SiO_2)_{1-x}$ films. This is in agreement with Raman scattering data obtained for as-deposited samples.

As it was mentioned the peak position of Raman band of the Si-ncs for $Si_x(Al_2O_3)_{1-x}$ in the samples with x>0.55 shifts slightly to high frequency side with the x decrease that cannot be caused by the change of crystallite sizes because the decrease of Si content should result in the decrease of Si crystallites and lead to opposite shift of Raman line. The observed shift is obviously caused by the decrease of amorphous Si phase content that is in agreement with the decrease of intensity of TA phonon of amorphous Si ($\omega_{TA\text{-}a\text{-}Si}$=150 cm^{-1}). Thus, the sizes of Si-ncs in $Si_x(Al_2O_3)_{1-x}$ films cannot be estimated from Raman data.

Another situation occurs in the $Si_x(SiO_2)_{1-x}$ films. With the x decrease the shift of the $\omega_{TO\text{-}nc\text{-}Si}$ to the lower wavenumbers occurs (Fig.1b, inset). Besides, the increase of full-width at half maximum of this phonon band is observed (not shown). The sizes of Si-ncs embedded in SiO_2 host can be estimated from the fitting of Raman scattering spectra. Based on such analysis the increase of Si-ncs mean size from ~2.7 nm to 6.0 nm was found for $Si_x(SiO_2)_{1-x}$ samples when the x increases from 0.3 to 0.5, whereas for x>0.5, Si-ncs size does not change practically. These results are in a good agreement with XRD data.

Obtained results showed also that mean size of Si-ncs in Al_2O_3 exceeds that for Si-ncs in SiO_2 for the films with same x values. One of the reasons of this phenomenon can be faster diffusion of Si in alumina than that in silica in the case when Si-ncs formation is determined by Si diffusion towards Si-nuclei and their Ostwald ripening. Another reason can be lower temperature required for phase separation in $Si_x(Al_2O_3)_{1-x}$ than that for $Si_x(SiO_2)_{1-x}$. In spite of the difference in Si-ncs sizes these films have one trait in common. For the samples with x>0.5 the mean Si-ncs sizes do not change with x. This can be connected with presence of amorphous Si inclusions in as-deposited films. In this case their crystallization can contribute to appearance of Si-nc besides the process of phase separation. For x>0.5 this contribution can be crucial. If these inclusions are big enough (that can be expected for high Si excess) the crystallite sizes will be determined by the temperature and duration of annealing only as for amorphous Si films crystallization. Indeed, rapid thermal annealing of $Si_x(Al_2O_3)_{1-x}$ samples results in the formation of smaller Si-ncs, but their mean size was found to be independent on x for x>0.5 [17].

Raman scattering spectra of annealed films showed also the higher relative contribution of amorphous Si phase in $Si_x(SiO_2)_{1-x}$ than in $Si_x(Al_2O_3)_{1-x}$. This can be due to lower temperature for the crystallization of amorphous Si clusters in Al_2O_3 host compared with that in SiO_2 and is in the agreement with the data of Ref. [12].

Obtained data show significant difference in PL properties of $Si_x(SiO_2)_{1-x}$ and $Si_x(Al_2O_3)_{1-x}$ films. For $Si_x(SiO_2)_{1-x}$ films, evolution of PL peak position versus x correlates with the variation of Si-ncs mean size. This allows ascribing it to exciton recombination in Si-ncs. Thus, in these films exciton recombination in Si-ncs is dominant radiative channel.

At the same time several radiative channels are observed in $Si_x(Al_2O_3)_{1-x}$ films. The investigation of temperature behavior of PL spectra showed that the peak positions and the intensities of PL components peaked at 2.06-2.15 eV and 1.65-1.77eV do not change with cooling [17]. This allowed ascribing them to radiative recombination of carriers through the defects of matrix and/or Si-ncs/host interface states. They are F-like centers in Al_2O_3 emitted at ~2.06 eV [22] and ~2.18 eV [21]. It is worth to note that PL components at ~1.65-1.77 eV and ~2.06 eV were observed only when Si-ncs are present in the film. This can be explained by their location near Si-ncs or at Si-ncs/host interface.

At the same time the contribution of near-infrared tail or band peaked at about 1.55 eV increases with cooling [17] that is typical feature of Si-ncs exciton PL band. However, its PL intensity is much lower than the emission of oxide-related defects contrary to that observed in $Si_x(SiO_2)_{1-x}$ films. This can be due to high number of non-radiative defects at Si-ncs/Al_2O_3 interface which, in particular, can appear due to mechanical stress in $Si_x(Al_2O_3)_{1-x}$ films.

Summary

In this work structural and luminescence properties of $Si_x(SiO_2)_{1-x}$ and $Si_x(Al_2O_3)_{1-x}$ films with different Si content prepared by magnetron sputtering on quartz substrate was compared. The formation of amorphous Si clusters upon deposition process was observed in both types of the films for the samples with x>0.3. The annealing treatment at 1150°C during 30 min results in formation of Si nanocrystallites (Si-ncs). Because of the presence of amorphous Si inclusions in as-deposited films two processes can contribute to their formation: the crystallization of existing inclusions and the process of phase separation at high temperatures. The first process can be responsible for independence of mean sizes of crystallites for x>0.5 that was observed in the both types of annealed films. At the same time a number of differences were found in structural and photoluminescence properties these films. The Si-nc sizes were found to be larger in $Si_x(Al_2O_3)_{1-x}$ films than that in $Si_x(SiO_2)_{1-x}$ counterparts with the same x values that can be caused by faster diffusion of Si in alumina than that in silica or by lower temperature required for phase separation in $Si_x(Al_2O_3)_{1-x}$ than that for $Si_x(SiO_2)_{1-x}$. Besides, Raman scattering spectra of annealed films showed the higher relative contribution of amorphous Si phase in $Si_x(SiO_2)_{1-x}$ than in $Si_x(Al_2O_3)_{1-x}$ as well as the presence of tensile stress in Si-nc embedded in $Si_x(Al_2O_3)_{1-x}$ films. The first can be caused by the lower temperature for the crystallization of amorphous Si clusters in Al_2O_3 host compared with that in SiO_2 while the second is due to mismatching between lattice parameters of fused quarts and the film. It is shown also that exciton recombination in Si-ncs is dominant radiative channel in $Si_x(SiO_2)_{1-x}$ films while the emission of oxide or Si/matrix interface -related defects dominates in $Si_x(Al_2O_3)_{1-x}$ films. This can be due to high number of non-radiative defects at Si-ncs/Al_2O_3 interface which, in particular, can appear due to mechanical stress in $Si_x(Al_2O_3)_{1-x}$ films.

Acknowledgements

This work was supported by the National Academy of Sciences (Ukraine), Ministry of Art and Science (Israel) and The National Center for Scientific Research (France).

References

[1] L.T. Canham, Silicon quantum wire array fabrication by electrochemical and chemical dissolution of wafers, Appl. Phys. Lett. 57 (1990) 1046-1048.

[2] V. Lehman, U. Gösele, Porous silicon formation: A quantum wire effect, Appl. Phys. Lett. 58 (1991) 856-858.

[3] T. Shimizu-Iwayama, S. Nakao, K. Saitoh, Visible photoluminescence in Si^+-implanted thermal oxide films on crystalline Si, Appl. Phys. Lett. 65 (1994) 1814-1816.

[4] X.Y. Chen, Y.F. Lu, L.J. Tang, Y.H. Wu, B.J. Cho, X.J. Xu, J.R. Dong, W.D. Song, Annealing and oxidation of silicon oxide films prepared by plasma-enhanced chemical vapor deposition, J. Appl. Phys. 97 (2005) 014913.

[5] L. Khomenkova, N. Korsunska, V. Yukhimchuk, B. Jumaev, T. Torchinska, A. Vivas Hernandez, A. Many, Y. Goldstein, E. Savir, J. Jedrzejewski, Nature of visible luminescence and its excitation in Si-SiO_x systems, J. Lumin. 102-103 (2003) 705-711.

[6] N. Baran, B. Bulakh, Ye. Venger, N. Korsunska, L. Khomenkova, T. Stara, Y. Goldstein, E. Savir, J. Jedrzejewski, The structure of Si–SiO_2 layers with high excess Si content prepared by magnetron sputtering, Thin Solid Films 517 (2009) 5468–5473.

[7] L. Khomenkova, N. Korsunska, T. Stara, Ye. Venger, C. Sada, E. Trave, Y. Goldstein, J. Jedrzejewski, E. Savir, Depth redistribution of components of SiOx layers prepared by magnetron sputtering in the process of their decomposition, This Solid Films 515 (2007) 6749–6753.

[8] G.G. Qin, X.S. Liu, S.Y. Ma, J. Lin, G.Q. Yao, X.Y. Lin, K.X. Lin, Photoluminescence mechanism for blue-light-emitting porous silicon, Phys. Rev. B 55 (1997) 12876-12879.

[9] L. Khomenkova, X. Portier, J. Cardin, F. Gourbilleau, Thermal stability of high-k Si-rich HfO_2 layers grown by RF magnetron sputtering, Nanotechnology 21 (2010) 285707 (10 pages).

[10] R.F. Steimle, R. Muralidhar, R. Rao, M. Sadd, C.T. Swift, J. Yater, B. Hradsky, S. Straub, H. Gasquet, L. Vishnubhotla, E.J. Prinz, T. Merchant, B. Acred, K. Chang, B.E. White Jr, Silicon nanocrystal non-volatile memory for embedded memory scaling, Microel. Reliab. 47 (2007) 585-592.

[11] T. Baron, A. Fernandes, J.F. Damlencourt, B. De Salvo, F. Martin, F. Mazen, S. Haukka, Growth of Si nanocrystals on alumina and integration in memory devices, Appl. Phys. Lett. 82 (2003) 4151-4153.

[12] A.N. Mikhaylov, A.I. Belov, A.B. Kostyuk, I.Yu. Zhavoronkov, D.S. Korolev, A.V. Nezhdanov, A.V. Ershov, D.V. Guseinov, T.A. Gracheva, N.D. Malygin, E.S. Demidov, D.I. Tetelbaum, Peculiarities of the formation and properties of light-emitting structures based on ion-synthesized silicon nanocrystals in SiO_2 and Al_2O_3 matrices, Physics of the Solid State (St. Petersburg, Russia) 54 (2012) 368-382.

[13] S. Yerci, U. Serincan, I. Dogan, S. Tokay, M. Genisel, A. Aydinli, R. Turan, Formation of silicon nanocrystals in sapphire by ion implantation and the origin of visible photoluminescence, J. Appl. Phys. 100 (2006) 074301 (5 pages).

[14] S. Núñez-Sánchez, R. Serna, J. García López, A.K. Petford-Long, M. Tanase, B. Kabius, Tuning the Er^{3+} sensitization by Si nanoparticles in nanostructured as-grown Al_2O_3 films, J. Appl. Phys. 105 (2009) 013118 (5 pages).

[15] L. Bi, J.Y. Feng, Nanocrystal and interface defects related photoluminescence in silicon-rich Al_2O_3 films, J. Lumin. 121 (2006) 95-101.

[16] http://www.horiba.com/scientific/products/ellipsometers/software/

[17] N. Korsunska, T. Stara, V. Strelchuk, O. Kolomys, V. Kladko, A. Kuchuk, B. Romanyuk, O. Oberemok, J. Jedrzejewski, P. Marie, L. Khomenkova, I. Balberg, Si-rich Al_2O_3 films grown by RF magnetron sputtering: structural and photoluminescence properties versus annealing treatment, Nanoscale Research Letters, 2013, accepted for publication, ID:1955309885820275.

[18] B.J. Jones, R.C. Barklie, Elecron paramagnetic resonance evolution of defects at the (100)Si/Al_2O_3 interface, J. Phys. D.: Appl. Phys. 38 (2005) 1178-1181.

[19] N. Korsunska, T. Stara, V. Strelchuk, O. Kolomys, V. Kladko, A. Kuchuk, L. Khomenkova, J. Jedrzejewski, I. Balberg, The influence of annealing on structural and photoluminescence properties of silicon-rich Al_2O_3 films prepared by co-sputtering. Physica E, 51 (2013) 115-119.

[20] S. Yin, E. Xie, C. Zhang, Z. Wang, L. Zhou, I.Z. Ma, C.F. Yao, H. Zang, C.B. Liu, Y.B. Sheng, J. Gou, Photoluminescence character of Xe ion irradiated sapphire, Nucl. Instr. Methods B 12-13 (2008) 2998-3001.

[21] Y. Song, C.H. Zhang, Z.G. Wang, Y.M. Sun, J.L. Duan, Z.M. Zhao, Photoluminescence of inert-gas ion implanted sapphire after 230-MeV Pb ion irradiation, Nucl. Instr. Methods B 245 (2006) 210-213.

[22] I. Dogan, I. Yildiz, R. Turan, PL and XPS depth profiling of Si/Al_2O_3 co-sputtered films and evidence of the formation of silicon nanocrystals, Physica E 41 (2009) 976-981.

Functional Nanomaterials and Devices VII
10.4028/www.scientific.net/AMR.854

Comparative Investigation of Structural and Optical Properties of Si-Rich Oxide Films Fabricated by Magnetron Sputtering
10.4028/www.scientific.net/AMR.854.117